A&A 498, L29–L32 (2009)
DOI: 10.1051/0004-6361/200911840

Astronomy & Astrophysics

Letter to the Editor

Propagating transverse waves in soft X-ray coronal jets

S. Vasheghani Farahani, T. Van Doorsselaere, E. Verwichte, and V. M. Nakariakov

Centre for Fusion, Space, and Astrophysics, Physics Department, University of Warwick, Coventry CV4 7AL, UK
e-mail: s.vasheghani-farahani@warwick.ac.uk

Received 12 February 2009 / Accepted 21 March 2009

ABSTRACT

Aims. The theoretical model for magnetohydrodynamic (MHD) modes guided by a field-aligned plasma cylinder with a steady flow is adapted to interpret transverse waves observed in solar coronal hot jets, discovered with Hinode/XRT in terms of fast magnetoacoustic kink modes.
Methods. Dispersion relations for linear magnetoacoustic perturbations of a plasma jet of constant cross-section surrounded by static magnetised plasma are used to determine the phase and group speeds of guided transverse waves and their relationship with the physical parameters of the jet and the background plasma. The structure of the perturbations in the macroscopic parameters of the plasma inside and outside the jet, and the phase relations between them are also established.
Results. We obtained a convenient expansion for the long wave-length limit of the phase and group speeds and have shown that transverse waves observed in soft-X-ray solar coronal jets are adequately described in terms of fast magnetoacoustic kink modes by a magnetic cylinder model, which includes the effect of a steady flow. In the observationally determined range of parameters, the waves are not found to be subject to either the Kelvin-Helmholtz instability or the negative energy wave instability, and hence they are likely to be excited at the source of the jet.

Key words. magnetohydrodynamics (MHD) – waves – Sun: corona – Sun: activity – Sun: magnetic fields

1. Introduction

Hot jets are often observed in the solar corona in the soft X-ray band as transient, collimated features with apparent high-velocity outflows in the direction of collimation (Shibata et al. 1992; Alexander & Fletcher 1999). Statistical analysis of jets observed with Yohkoh/SXT (e.g., Shimojo et al. 1996) revealed that most jets are associated with flaring energy releases, mainly small flares and microflares. The typical observed lengths of hot jets, defined as the distance from base to where its intensity drops below some certain value, are in the range of between a few tens and several hundred thousand km, and their diameters are one to two orders of magnitude smaller. The typical aspect ratio of length to width was measured to be about ten. The lifetime is typically in the range from several minutes to an hour. About half of the observed jets showed a constant width, and about a third had a width decreasing with height. The observed flow speeds are several hundred km s^{-1}, reaching in some cases about a thousand km s^{-1}. The estimate of the speed is affected by the projection effect, and by the obvious difficulties connected with the measurement of a physical speed with an imaging instrument. The majority of jets are situated over regions of mixed polarity. Shibata et al. (1992) suggested that hot jets are associated with reconnection outflows. Numerical MHD modelling (Yokoyama & Shibata 1995) showed that an anemone jet could result from the interaction of an emerging magnetic flux with a vertical or oblique background magnetic field.

Progress in the study of hot jets has been achieved using Hinode/XRT (Golub et al. 2007), which allows us to detect up to 10 jets per hour (Cirtain et al. 2007) with an average temperature of about 6 MK. Such a frequency of appearance is an order of magnitude greater than determined with SXT. The typical lifetime of jets was found to be about 100–1500 s, which is consistent with the results obtained for the lifetime of jets with SXT. The speeds of the outflows were estimated to be in the range from 200 to 800 km s^{-1}. Hot jets observed in soft X-rays precede cool jets observed in the optical band (Nishizuka et al. 2008).

In addition, it became possible to study the fine structure of the jets, revealing the presence of transverse oscillations (Cirtain et al. 2007), which were periodic displacements in the jet axis with a period of about 200 s and a displacement amplitude of about 4000 km. The latter value is half of the given value for the peak-to-peak magnitude. The question arises about the nature of these waves.

Transverse oscillations have been known to exist in the corona for a long time. For example, 300 s, 80 s, and 43 s periodicities were found by Koutchmy et al. (1983) in the Doppler shift of the green coronal line, and interpreted as standing kink waves by Roberts et al. (1984). A number of observational examples of transverse (kink) standing waves has been found with the EUV imager TRACE in coronal loops (Aschwanden et al. 1999; Nakariakov et al. 1999). Propagating transverse waves were also observed in flaring supra-arcade regions by Verwichte et al. (2005) with TRACE. The observed periods were about 90–220 s. The observed apparent phase speeds were several hundred km s^{-1}, decreasing with height. These waves are interpreted as propagating, fast magnetoacoustic kink waves guided by a plasma structure. Waves of short period, about 6 s, were detected in eclipse visible light observations of coronal loops with the SECIS instrument by Williams et al. (2001). The phase speed was about 2000 km s^{-1}. It was shown that the observed variation in the emission intensity was consistent with the modulation of the observed column depth of the loop by a kink wave (Cooper et al. 2003). Propagating transverse waves were

investigated by Tomczyk et al. (2007) in the visible light with the COMP instrument. The detected period was about 300 s, and the phase speed 1000–4000 km s^{-1}. Van Doorsselaere et al. (2008) demonstrated that the transverse perturbations localised in the perpendicular direction, such as all observational examples found so far, can propagate along the magnetic field only in the presence of a guiding structure, i.e., a loop or a jet. The guiding is caused by the refraction or reflection of fast magnetoacoustic waves from a gradient in the fast speed. A similar guiding effect takes place when there is a gradient of the steady flow speed in the structure (Nakariakov et al. 1996). Kink waves also were observed in cool dense coronal filaments (Ofman & Wang 2008).

The theoretical model of MHD waves guided by a plasma structure of steady flow was developed by Goossens et al. (1992) and Terra-Homem et al. (2003) for the cylindrical geometry and by Nakariakov & Roberts (1995) for the slab geometry. The main new feature introduced by the flow was the modification of the dispersion relations and wave-flow interaction effects associated with negative energy (Joarder et al. 1997). The latter can cause instabilities at steady flow speeds well below the KHI threshold, which occurs when the flow-speed shear exceeds the Alfvén speed by a factor of about two (Ruderman et al. 1996).

The aim of this Letter is to adapt the theoretical model for MHD waves guided by a plasma cylinder with a steady flow in interpreting the transverse waves observed by Cirtain et al. (2007) in soft X-ray coronal jets. We do not consider the jet formation or collimation, but restrict ourselves to the analysis of linear MHD perturbations of the observed plasma configuration. We demonstrate by expansions of the dispersion relation in the long wave-length limit that the observed properties of waves are consistent with guided, fast magnetoacoustic, kink waves.

2. Model and dispersion relations

We consider a hot jet as a uniform cylinder of radius a with the equlibrium, internal, magnetic field $B_0\hat{\mathbf{z}}$ parallel to the axis of the jet. Outside the cylinder, the magnetic field is $B_e\hat{\mathbf{z}}$. The gas pressure and density within the cylinder are P_0 and ρ_0, respectively, and outside the cylinder, they are P_e and ρ_e, respectively. Total pressure balance implies that $P_0 + B_0^2/2\mu = P_e + B_e^2/2\mu$, where μ is the magnetic permeability. Hence, the densities ρ_0 and ρ_e are related by

$$\frac{\rho_e}{\rho_0} = \frac{2\,c_0^2 + \gamma\,v_{A0}^2}{2\,c_e^2 + \gamma\,v_{Ae}^2}, \tag{1}$$

where $c_0 = (\gamma\,P_0/\rho_0)^{1/2}$ and $v_{A0} = B_0/\sqrt{\mu\rho_0}$ are the sound and Alfvén speeds inside the cylinder, respectively, $c_e = (\gamma\,P_e/\rho_e)^{1/2}$ and $v_{Ae} = B_e/\sqrt{\mu\rho_e}$ are the corresponding speeds outside, and γ is the ratio of the specific heats. Inside the cylinder, there is a field-aligned steady flow with $\vec{V} = U_0\hat{\mathbf{z}}$. Outside the jet, there is no steady flow, $U_e = 0$. In both regions, the plasma-β is taken to be below unity.

We consider linear *helical* perturbations to the steady-flow equilibrium, of azimuthal wave number $m = 1$ because they are the only ones perturbating the jet axis. Following Goossens et al. (1992), the general dispersion relation linking the frequency ω to the longitudinal wave number k of an $m = 1$ mode is

$$\frac{\rho_0}{\rho_e}\,\frac{(k^2\,v_{A0}^2 - \Omega_0^2)}{(k^2\,v_{Ae}^2 - \omega^2)}\,\frac{m_e}{n_0}\,\frac{K_1'\,(m_e\,a)}{K_1\,(m_e\,a)} = \frac{J_1'\,(n_0\,a)}{J_1\,(n_0\,a)}, \tag{2}$$

where $\Omega_0 = \omega - U_0\,k$ is the Doppler-shifted frequency,

$$n_0^2 = -\frac{(k^2c_0^2 - \Omega_0^2)(k^2\,v_{A0}^2 - \Omega_0^2)}{(c_0^2 + v_{A0}^2)(c_{T0}^2\,k^2 - \Omega_0^2)}, \quad c_{T0}^2 = \frac{c_0^2\,v_{A0}^2}{c_0^2 + v_{A0}^2}, \tag{3}$$

and

$$m_e^2 = \frac{(k^2c_e^2 - \omega^2)(k^2\,v_{Ae}^2 - \omega^2)}{(c_e^2 + v_{Ae}^2)(c_{Te}^2\,k^2 - \omega^2)}, \quad c_{Te}^2 = \frac{c_e^2\,v_{Ae}^2}{c_e^2 + v_{Ae}^2}, \tag{4}$$

where C_{T0} and C_{Te} are the inside and outside tube speeds, respectively. Equation (2) is a transcendental implicit algebraic equation that does not have exact analytical solutions.

Since the wavelengths of transverse perturbations observed by Cirtain et al. (2007) are significantly longer than the radius a of the jet, it is sufficient to consider the limiting case of $|k|\,a \ll 1$. From Eq. (2), the phase and group speeds can be approximated by the explicit expressions:

$$\omega/k \approx v_G + \alpha\,k^2a^2\ln(|k|a), \tag{5}$$

$$\mathrm{d}\omega/\mathrm{d}k \approx v_G + 3\alpha\,k^2a^2\ln(|k|a), \tag{6}$$

$$v_G = \frac{\rho_0\,U_0}{\rho_0 + \rho_e} + v_{cm}, \tag{7}$$

$$\alpha = -\frac{1}{2}\frac{\rho_0(v_{A0}^2 - (v_G - U_0)^2)(v_{Ae}^2 - v_G^2)}{(\rho_0 + \rho_e)\,v_{Ae}^2\,v_{cm}}, \tag{8}$$

$$v_{cm} = \sqrt{c_k^2 - \frac{\rho_0\rho_e}{(\rho_0 + \rho_e)^2}\,U_0^2}, \; c_k = \sqrt{\frac{\rho_0\,v_{A0}^2 + \rho_e\,v_{Ae}^2}{\rho_0 + \rho_e}}. \tag{9}$$

For $k = 0$, Eq. (5) reduces to $\omega/k \approx v_G$, which is the result found by Goossens et al. (1992). For $U_0 = 0$, Eq. (5) becomes

$$\frac{\omega}{k} = c_k\left\{1 + \frac{\rho_0\rho_e\left(v_{Ae}^2 - v_{A0}^2\right)\left(v_{Ae}^2 - c_k^2\right)}{2(\rho_0 + \rho_e)^2v_{Ae}^2c_k^2}k^2a^2\ln(|k|\,a)\right\}, \tag{10}$$

which coincides with the expression given in Edwin & Roberts (1983), but here instead of the modified second-order Bessel function, we use a more convenient logarithmic expression as its asymptotic equivalent. Using the observational fact that the jet is significantly denser than the background plasma (Culhane et al. 2007), $\rho_e/\rho_0 \ll 1$, we can further simplify Eqs. (5)–(9) to,

$$v_G \approx U_0 + v_{A0}\sqrt{1 + (B_e/B_0)^2}, \quad \alpha \approx \frac{v_{A0}}{2}\frac{(B_e/B_0)^2}{\sqrt{1 + (B_e/B_0)^2}}\cdot \tag{11}$$

In Fig. 1, the dependence of the phase and group speeds on the wave number is shown, which is calculated numerically with the use of the full dispersion relation of Eq. (2), and analytically with the use of asymptotic expressions in Eqs. (5)–(9) and (11). All three approaches show satisfactory consistency. Both asymptotic expressions are independent of the sound speeds inside and outside the jet.

Linear perturbations of macroscopic physical parameters in the kink wave are expressed in terms of the divergence of the plasma velocity perturbation, $\Delta(r)$ as

$$\rho = -\frac{\rho_{\{0,e\}}}{\Omega}\Delta(r)\,\sin\Theta, \quad B_z = -\frac{B_{\{0,e\}}}{\Omega}\Delta(r)\,\sin\Theta,$$

$$v_\theta = \frac{v_A^2}{(\Omega^2 - k^2\,v_A^2)\,r}\Delta(r)\,\sin\Theta,$$

$$B_\theta = -\frac{k\,B_{\{0,e\}}\,v_A^2}{(\Omega^2 - k^2\,v_A^2)\Omega\,r}\Delta(r)\,\sin\Theta,$$

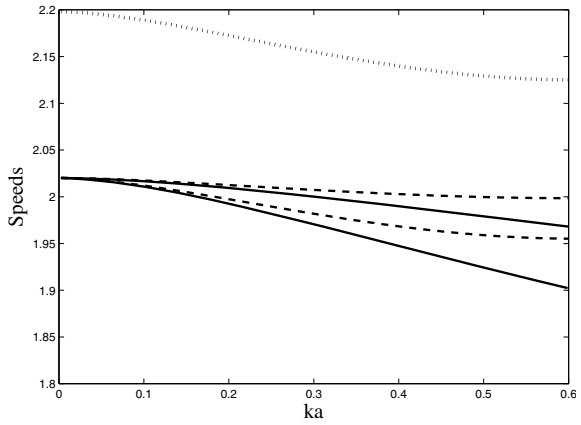

Fig. 1. Dependence of the phase and group speeds of the kink mode upon the wave number. The speeds are normalised to the Alfvén speed inside the jet, and the wave number to the reciprocal of the jet radius. The solid lines correspond to the numerical solution of the exact dispersion relation, the *upper* and *lower* being the phase and group speeds, respectively. The dashed lines correspond to the asymptotic expressions utilising the limit $ka \to 0$, where the higher and lower curve are the phase and group speeds, respectively. The dotted line shows the asymptotic expression with both $ka \to 0$ and $\rho_e/\rho_0 \to 0$. In the calculations, $U_0 = 580\ \mathrm{km\,s^{-1}}$, $V_{Ae} = 2400\ \mathrm{km\,s^{-1}}$, $V_{A0} = 800\ \mathrm{km\,s^{-1}}$, $c_0 = 360\ \mathrm{km\,s^{-1}}$, $c_e = 120\ \mathrm{km\,s^{-1}}$, and $\rho_e/\rho_0 = 0.13$.

$$v_r = \frac{v_A^2}{(k^2 v_A^2 - \Omega^2)} \frac{\mathrm{d}}{\mathrm{d}r}\Delta(r) \cos\Theta,$$
$$B_r = -\frac{v_A^2\, k\, B_{\{0,e\}}}{(k^2 v_A^2 - \Omega^2)\Omega} \frac{\mathrm{d}}{\mathrm{d}r}\Delta(r) \cos\Theta, \quad (12)$$

where $\Theta = \omega t + \theta - kz$, $\Delta(r) = A_0 J_1(n_0 r)$ inside the jet, $r < a$ and $\Delta(r) = A_0 J_1(n_0 a) K_1(m_e r)/K_1(m_e a)$ outside it, where A_0 is the amplitude of the perturbations. The z component of the velocity perturbations is zero. The transverse perturbations are *essentially* compressible, since they perturb the plasma density and the divergence of the velocity.

The relations in Eq. (12) together with the dispersion relations provide a complete description of transverse perturbations guided by a field-aligned plasma jet. It can be used in the forward modelling of the observational manifestation of this phenomenon. The emission intensity recorded by XRT is proportional to the integration of the plasma density squared along the line-of-sight. First, a 4D (spatial 3D and time) data cube of the plasma density in the oscillating jet is created. Specifying the line-of-sight, we obtain a time sequence of 2D images (snapshots), showing the distribution of intensity to be observed. Some random variations in the intensity were added to represent e.g., the electronic noise and other processes missing in the model. The jet radius was 5 pixels, which should correspond to a jet of radius 3.6 Mm observed with Hinode/XRT. In Fig. 2, we show results for the forward modelling of an off-limb coronal loop with a dense radial jet, as it would be seen with Hinode/XRT, with the jet experiencing transverse oscillations described by Eq. (12). Different snapshots correspond to different phases of the oscillation. The snapshots agree well with the observational results of Cirtain et al. (2007). Figure 3 shows a time-distance plot of the oscillation. A one-pixel-wide slit across the oscillating jet is selected, and the intensity distribution along the slit is determined in each snapshot. The measure of intensity along the slit is plotted as a column. By stacking the columns from sequential snapshots along the horizontal axis of the plot, a representation of the intensity variation in distance and time is created.

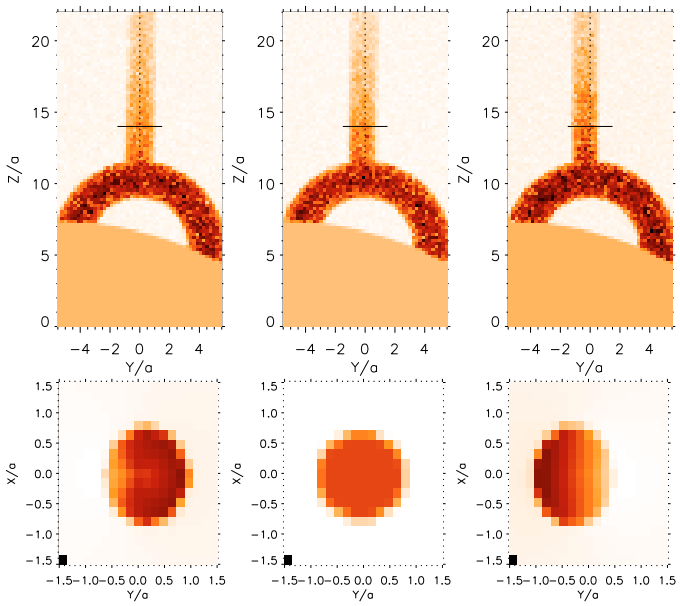

Fig. 2. Forward modelling of transverse oscillations of a soft X-ray jet directed from an off-limb coronal loop seen by Hinode/XRT (with the pixel size about 727 km, the inverse colour table is used). The region in the bottom of the top row figures shows the solar disk. The jet is the vertically positioned linear feature directed from the loop. The *top row* shows snapshots of the side view of an oscillating jet at times $t = 0$, $t = 0.125\,P$, and $t = 0.25\,P$, where P is the period of the oscillations. The jet oscillates in the plane perpendicular to the line-of-sight. The perturbation of the jet corresponds to the analytical solution of linearised MHD. The *bottom row* shows the density distribution over the jet cross-section at the location of the black slit indicated in the corresponding *top panels*. The jet radius is 3.6 Mm, and the oscillation displacement amplitude is 1.5 Mm, and other parameters as in Fig. 1.

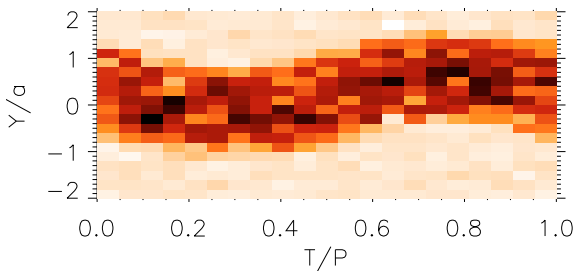

Fig. 3. Time-distance plot of the oscillating jet, as it would be seen by Hinode/XRT. The slit position is shown in Fig. 2. The spatial axis is normalised to the loop radius, and the time axis is normalised to the oscillation period. The perturbation of the jet corresponds to the analytical solution of the linearised MHD. The parameters of the simulation are the same as in Fig. 2.

3. Discussion and conclusions

We have demonstrated that transverse waves observed in soft X-ray solar coronal jets (Cirtain et al. 2007) are adequately described in terms of fast magnetoacoustic kink ($m = 1$) modes of a straight magnetic cylinder embedded in a magnetic environment. It is shown that these waves are collective, since they are coherent perturbations of all magnetic surfaces inside the jet, and compressible, since the flow-perturbation divergence is finite. Phase and group speeds are determined by the density contrast

of the jet, the flow speed, and the internal and external Alfvén speeds. Forward modelling performed with the use of theoretically determined phase relations was found to be consistent with the observational findings obtained with Hinode/XRT.

The above expressions are written for the azimuthal mode number $m = 1$. However, a transverse displacement of the axis of the cylinder, such as the transverse motion of the jet, can, in general, have two opposite senses, $m = \pm 1$. The azimuthal modes $m = \pm 1$ manifest themselves as a cork-screwing motion travelling along the cylinder. The $m = +1$ mode has a right-hand twist, whereas the $m = -1$ mode has a left-hand twist. Physically, the plane-polarised wave can be constructed by superposition of the $m = +1$ mode with an $m = -1$ mode of an equal amplitude. An elliptical cork-screwing motion may be constructed by superposing $m = +1$ and $m = -1$ modes with unequal amplitudes. However, it is impossible to distinguish observationally between a pure $m = \pm 1$ mode or a superposition of these modes. Most of the solar observation facilities (except for STEREO) observe only the plane of the sky displacements (imaging telescopes) or the line-of-sight velocities (spectrographs). As such, it is only possible to measure the projected motion of the jet. It is impossible to quantify the motion in the other direction and thus to assess the nature (pure or superposition) of the observed oscillation. For Fig. 2 we have displayed the plane polarisation, but it is indistinguishable from that of an $m = \pm 1$ mode.

If there is a variation in the Alfvén or flow speed across the jet, the kink perturbations are subject to resonant absorption. Using Eq. (76) from Goossens et al. (1992), we estimate the damping time $t_{\rm damp}$ of the kink oscillations in a jet for the parameters used in Figs. 1 and 2 as $t_{\rm damp}/s \approx 640(a/\delta)$, where $a/\delta > 1$ is the ratio of the jet radius a to the width δ of the resonant layer and the wave phase speed coincides with the local Alfvén speed. For the observed period of about 200 s, the damping time is several times longer than the wave period, justifying the model.

The jets are observed at heights of up to 100 Mm, while for plasmas of temperature e.g., 10 MK, the density scale height is about 500 Mm. This comparison allows us to ignore the stratification. However, in a more detailed study, effects of stratification and longitudinal structuring should be considered. It is unclear how the wave evolves past the physical extent of the jet, which will depend on the transverse structuring that is not visible in the observations.

The origin of the transverse oscillations of soft X-ray jets has not yet been understood. One possible candidate mechanism could be the Kelvin-Helmholtz instability (Ferrari et al. 1981). For a plasma cylinder of the observed geometry with the typical values of the Alfvén speed ($v_{\rm Ae} = 3v_{\rm A0}$, which correspond to the density contrast $\rho_{\rm e}/\rho_0 \cong 0.13$), the instability threshold value of the steady flow speed is $U_0 = 4.47v_{\rm A0}$. Since the observed values of the jet speeds do not exceed the Alfvén speed inside the jet, the instability threshold is not reached and this possibility should be excluded. Another option is related to negative energy wave instabilities. However, according to Joarder et al. (1997) in the considered situation, sub-Alfvénic flow speeds can lead to the instability of longitudinal modes only, which does not explain the generation of the transverse perturbations. Also, the periodicity could appear because of geometric dispersion (Roberts et al. 1984; Murawski & Roberts 1994). However, the typical wavelength generated by this mechanism would be comparable to the jet diameter and hence we exclude this option too. Consequently, we deduce that the observed transverse waves are excited somewhere at the origin of the jet, possibly by oscillatory magnetic reconnection (Murray et al. 2009), and then propagate according to the dispersion and phase relations discussed above. Observation of transverse waves guided by soft X-ray jets is interesting in terms of coronal seismology. According to Eqs. (5) and (11), the phase speed of these waves is about $\omega/k \approx v_{\rm G} \approx U_0 + v_{\rm A0}\sqrt{1 + (B_{\rm e}/B_0)^2}$, which is determined by the flow speed and the Alfvén speed inside the jet. Another constraint is given by the equilibrium condition (Eq. (1)), which can be rewritten as $\rho_{\rm e}/\rho_0 \approx (6/5 + v_{\rm A0}^2/c_0^2)/(v_{\rm Ae}^2/c_0^2)$, where we have assumed that the external β is very small and $\gamma = 5/3$. These expressions contain observables: the phase speed of transverse waves, the flow speed (Cirtain et al. 2007), the density-contrast ratio (which can be obtained from the emission-measure contrast) and the sound speed (which is connected with the temperature). The use of the observed values in the theoretical constraints allows us to estimate the internal and external Alfvén speeds, and the magnetic fields.

References

Alexander, D., & Fletcher, L. 1999, Sol. Phys., 190, 167
Aschwanden, M. J., Fletcher, L., Schrijver, C. J., & Alexander, D. 1999, ApJ, 520, 880
Cirtain, J. W., Golub, L., Lundquist, L., et al. 2007, Science, 318, 1580
Cooper, F. C., Nakariakov, V. M., & Williams, D. R. 2003, A&A, 409, 325
Culhane, L., Harra, L. K., Baker, D., et al. 2007, PASJ, 59, 751
Edwin, P. M., & Roberts, B. 1983, Sol. Phys., 88, 179
Ferrari, A., Trussoni, E., & Zaninetti, L. 1981, MNRAS, 196, 1051
Golub, L., Deluca, E., Austin, G., et al. 2007, Sol. Phys., 243, 63
Goossens, M., Hollweg, J. V., & Sakurai, T. 1992, Sol. Phys., 138, 233
Joarder, P. S., Nakariakov, V. M., & Roberts, B. 1997, Sol. Phys., 176, 285
Koutchmy, S., Zhugzhda, I. D., & Locans, V. 1983, A&A, 120, 185
Murawski, K., & Roberts, B. 1994, Sol. Phys., 151, 305
Murray, M. J., van Driel-Gesztelyi, L., & Baker, D. 2009, A&A, 494, 329
Nakariakov, V. M., & Roberts, B. 1995, Sol. Phys., 159, 213
Nakariakov, V. M., Roberts, B., & Mann, G. 1996, A&A, 311, 311
Nakariakov, V. M., Ofman, L., Deluca, E. E., Roberts, B., & Davila, J. M. 1999, Science, 285, 862
Nishizuka, N., Shimizu, M., Nakamura, T., et al. 2008, ApJ, 683, L83
Ofman, L., & Wang, T. J. 2008, A&A, 482, L9
Roberts, B., Edwin, P. M., & Benz, A. O. 1984, ApJ, 279, 857
Ruderman, M. S., Verwichte, E., Erdelyi, R., & Goossens, M. 1996, J. Plasma Phys., 56, 285
Shibata, K., Ishido, Y., Acton, L. W., et al. 1992, PASJ, 44, L173
Shimojo, M., Hashimoto, S., Shibata, K., et al. 1996, PASJ, 48, 123
Terra-Homem, M., Erdélyi, R., & Ballai, I. 2003, Sol. Phys., 217, 199
Tomczyk, S., McIntosh, S. W., Keil, S. L., et al. 2007, Science, 317, 1192
Van Doorsselaere, T., Brady, C. S., Verwichte, E., & Nakariakov, V. M. 2008, A&A, 491, L9
Verwichte, E., Nakariakov, V. M., & Cooper, F. C. 2005, A&A, 430, L65
Williams, D. R., Phillips, K. J. H., Rudawy, P., et al. 2001, MNRAS, 326, 428
Yokoyama, T., & Shibata, K. 1995, Nature, 375, 42